LA-UR-90-3210

CONF-900926--1

Los Alamos National Laboratory is operated by the University of California for the United States Department of Energy under contract W-7405-ENG-36

LA-UR--90-3210

DE91 000222

TITLE: MEASUREMENT OF THE ABSOLUTE CROSS SECTION FOR MULTIPHOTON IONIZATION OF ATOMIC HYDROGEN AT 248 NM

AUTHOR(S): George A. Kyrala P-1
T. David Nichols P-1

SUBMITTED TO: Fifth International Conference on Multiphoton Processes
CEA, Institut de Recherche Fundamentale
Saclay, Paris
FRANCE

September 24-28, 1990

DISCLAIMER

This report was prepared as an account of work sponsored by an agency of the United States Government. Neither the United States Government nor any agency thereof, nor any of their employees, makes any warranty, express or implied, or assumes any legal liability or responsibility for the accuracy, completeness, or usefulness of any information, apparatus, product, or process disclosed, or represents that its use would not infringe privately owned rights. Reference herein to any specific commercial product, process, or service by trade name, trademark, manufacturer, or otherwise does not necessarily constitute or imply its endorsement, recommendation, or favoring by the United States Government or any agency thereof. The views and opinions of authors expressed herein do not necessarily state or reflect those of the United States Government or any agency thereof.

By acceptance of this article, the publisher recognizes that the U S Government retains a nonexclusive, royalty-free license to publish or reproduce the published form of this contribution, or to allow others to do so, for U S Government purposes

The Los Alamos National Laboratory requests that the publisher identify this article as work performed under the auspices of the U S Department of Energy

Los Alamos National Laboratory
Los Alamos, New Mexico 87545

FORM NO. 836 R4
ST. NO. 2629 5/81

DISTRIBUTION OF THIS DOCUMENT IS UNLIMITED

MASTER

Measurement of the Absolute Cross Section for Multiphoton Ionization of Atomic Hydrogen at 248 nm

George A. Kyrala and T. David Nichols
Physics Division
Los Alamos National Laboratory
Los Alamos, NM 87544

ABSTRACT

We present measurements of the absolute rates for multiphoton ionization of the ground state from atomic hydrogen by a linearly polarized, subpicosecond KrF laser pulse at a wavelength of 248 nm. A laser crossed atomic beam technique is used. The irradiance was varied from $3x10^{12}$ w/cm^2 to $2x10^{14}$ w/cm^2 and three above threshold ionization peaks were observed. The measured rate for total electron production is less than predicted by the numerical and perturbation calculations, but significantly higher than calculated by the Reiss and Keldysh methods.

INTRODUCTION

The interaction of atomic hydrogen with an intense laser field is one of the most fundamental tests of the features of multiphoton ionization (MPI) and above threshold ionization (ATI).

Several theoretical calculations of multiphoton ionization of atomic hydrogen have been published.[1-12] There are simple perturbative calculations that include intermediate states to some order[2,3,4,5,9,10] and those that employ Volkov states as the final states without including any intermediate states,[1,6,8]. There are also calculations that simulate the atom-radiation field by Floquet states[7] and those that use time dependent three dimensional calculations with direct numerical integrations of the Schroedinger equation[11,21].

Very few experiments have been performed on the multiphoton ionization of atomic hydrogen[12,13,14,15]. No experiment has been performed for single photon ionization. The earliest experiment by LuVan et al.[12] used 530 nm light and measured the ion yield resulting in rates 720 times greater than those from perturbation theory. They claimed the difference was due to the multimode nature of their laser beam. Later, three photon resonant ionization was measured by Kelleher et al.[13], but they were interested in the stark shift rather than the rate for ionization. Muller et al.[14] observed ATI peaks in the case of three photon ionization using two applied radiation fields, but again no rates were measured.

Wolff et al.[15] measured the angular distribution of the ATI peaks of atomic hydrogen at 1048, 532 and 355 nm. They, however, concentrated on the angular distribution features of the ionization.

In this work we concentrated on measuring the absolute cross section for 3 photon non-resonant ionization of atomic hydrogen by 248 nm linearly polarized light. Figure 1 shows the relevant energy diagram of the system. The main feature of this work is the few photon nature of the process and the absence of intermediate excited states. We had hoped to observe channel closing when the irradiance exceeded 180 TW/cm^2, but we found that the contribution from the low irradiance part of the focal volume masked that effect.

DESCRIPTION OF THE EXPERIMENT

1. Overview: In this experiment, we measured the number of ATI electrons produced at the intersection of an atomic hydrogen beam and a focused laser beam. We identified these electrons and measured their energies with an electron time of flight (TOF) spectrometer. An ultrahigh vacuum system minimized the electron signals from ionization of background gases, principally hydrogen molecules and water. The density of hydrogen atoms in the interaction region was measured with a residual gas analyzer (RGA) to be 10^9 to 10^{10} atoms/cm^3 depending on the operation of the source. An estimate from the measured gas flow rate and from kinetic theory confirmed these results. The peak irradiance at the center of the interaction region (I_0) was varied over the range 10^{12} to 10^{14} W/cm^2 using beamsplitters and reflective neutral density filters. These peak irradiances correspond to peak ponderomotive potentials (V_p) of 0.006 to 0.6 eV.

2. Laser and optical system: The laser system used for this work has been described elsewhere[16]. Briefly, it consists of a front end which produces a 248 nm pulse, followed by two single pass KrF gas discharge amplifiers. The laser output energy was typically 25 mJ, with a repetition rate of 5 Hz. The pulse length was 600 fsec FWHM, as measured by two-photon ionization of NO with a fitted sech^2(t) pulse shape. The product of the temporal and spectral widths was two to three times the product for a transform limited pulse. The beam was linearly polarized.

A schematic diagram of the experimental configuration is shown in Figure 2. A diffraction limited, 50 mm diameter, f/20 off-axis parabolic mirror focused the circular laser beam, of uniform irradiance, to a spot at the center of the interaction region. The laser beam exited through a beam dump channel and was collected in a Joulemeter. The atomic hydrogen beam entered the target chamber normal to the axis of the laser beam and to the axis of the electron TOF spectrometer.

The energy in the laser beam was varied by using mirrors with different reflectances and reflective neutral density filters, thus changing the pulse shape and irradiance distribution as little as possible. The peak irradiance at focus (I_0) could be varied from 10^{12} W/cm^2 to 2×10^{15} W/cm^2. We did not use the highest

available irradiance because all of the atoms in the center of the interaction region would ionize during the rising edge of the pulse, and none experienced the peak field strength.

3. Electron TOF spectrometer: Electrons generated at the laser focus were collected and their energy was analyzed using an electron time of flight spectrometer with 2π collection angle. The electron spectrometer was based on the Kruit and Read design[17] but used a permanent magnet rather than an electromagnet. A retarding potential could be placed on a grid which enclosed the drift region to increase the flight time, to improve the resolution, and to discriminate against low energy electrons. The electrons were detected by a two stage chevron microchannel plate electron multiplier (MCP). A transient recorder digitized the MCP signal with a sampling period of 10 nsec. After each laser pulse, the spectrum from the digitizer and the energy from the Joulemeter were recorded. The spectrum was binned and added together. The bin width was 3% of the average laser energy. The resolution of the spectrometer was measured to be 80 meV FWHM at 1.4 eV ($\triangle E/E = 0.06$).

4. Atomic hydrogen source: Figure 3 is a schematic diagram of the interaction region. The atomic hydrogen was produced by flowing molecular hydrogen through a Pyrex tube placed at the center of a 35 Mhz cavity[18]. The tube was water cooled to 20°C to minimize recombination on its surface. Atomic hydrogen effused from a 18 mm long, 1 mm diameter Pyrex tube and was collimated by a 1 mm diameter Teflon coated skimmer. The skimmer also acted as a differential pumping aperture between the source region and the interaction region. Ultraviolet light from the discharge was optically blocked by a small kink in the exit tube.

5. Alignment and focusing system: A 50 μm diameter pinhole was aligned to the center of the hydrogen beam, the axis of the collecting magnet, and the center of the electron TOF spectrometer. A collimated HeNe red beam was aligned collinear with the 248 nm beam. The red beam was focused to the center of the pinhole. Since both red and UV beams used the same reflecting optics, both beams were pointed and focused to the same point.

6. Vacuum system: The base vacuum of the interaction chamber was better than 5×10^{-9} Torr. When the atomic hydrogen beam was on, the pressure around the interaction region increased to 9×10^{-8} Torr. The chamber containing the discharge tube was maintained at a pressure of 1.6×10^{-6} Torr with the discharge on. This minimized the effusion of molecular hydrogen into the interaction region. The hydrogen beam was monitored on axis with a quadrupole residual gas analyzer. The analyzer measured the partial pressures of the impurities and the absolute dissociation fraction in the hydrogen beam.

7. Irradiance at focus: Irradiance in the interaction region was determined by measuring E_L the total energy of each laser pulse, the average length of the pulses, and the average radius of the beam. To obtain the average radius, measurements of the energy passing through a 25 micrometer diameter pinhole were fit to a modified gaussian model for the beam. This model describes a beam in which the longitudinal modes are locked together (the sech^2 time dependence), but many transverse modes, that can be expanded in a sum of many Hermite-Gaussian polynomials,[19] may be present. The model is:

$$I(r,z,t) = I_0\left\{\frac{W_0}{W(z)}\right\}^2 \mathrm{sech}^2\left(\frac{2t}{T_p}\right) \exp\left\{-2\left(\frac{r}{W(z)}\right)^2\right\} \qquad (1)$$

where W(z) is the spot radius at a distance z and I_0 the peak irrdiance is:

$$W(z)^2 = W_0^2\left\{1+\left(\frac{M^2\lambda z}{\pi W_0^2}\right)^2\right\}, \quad I_0 = \frac{2E_L}{T_p \pi W_0^2}, \qquad (2)$$

where r and z are cylindrical spatial coordinates, t is time, I_0 is the peak irradiance, T_p = 1.14 x pulse length (FWHM), and the wavelength λ equals 248 nm. The parameters to be determined are: W_0, the measured Gaussian waist radius, where the irradiance is $1/e^2$ of the irradiance on the axis (r = 0), and M^2, a measure of how many times diffraction limited the focus is.[20] M^2 is related to the waist radius w_0 of a diffraction limited focus by $W_0 = M^2 w_0$. Thus a TEM_{00} single-mode beam focused with a perfect lens will have $M^2 = 1$. M^2 also measures how quickly the beam expands with axial distance from the waist (z). Our measurements (see Figure 4 for a radial scan at best focus with a 25 micrometer aperture) indicated that the beam, after passing through our optical system, can be described by the values: T_p = 700±50 fsec, W_0 = 35+5/-2 μm, and M^2 = 5.8±0.2.

The measured value of W_0 = 35 μm represents the best performance. Occasionally, the waist radius changed to 45 μm, or oscillates between these values.

ELECTRON SPECTRUM

The measured electron spectrum shows few ATI peaks, even at the highest available irradiance (2×10^{15} W/cm^2). Two spectra are shown in Figure 5 under the same laser conditions: one for molecular hydrogen with the RF discharge off, and one for atomic hydrogen when the RF discharge was on. The molecular peaks decrease when the discharge is turned on to produce atomic hydrogen. The relative decrease of this peak gives a measure of the degree of dissociation of

the discharge. Other peaks from contaminants such as water and nitrogen are easily resolvable, and do not contribute to the measured rates for production for the first hydrogen ATI peak.

COMPARISON BETWEEN THE CALCULATED AND THE MEASURED THREE-PHOTON RATES

In order to compare the experimental results with the theoretical calculations, we fold the theoretical calculations with the experimental parameters to predict a signal. The focal volume is divided into shells that experience the same temporal history, i.e., contours of equal peak irradiance, then every atom within a given contour experiences the same temporal history. At that given characteristic peak irradiance I_p, the hydrogen density $N_h(I_p,t)$ is related to the electron density and the transition rate for k photons W_k by:

$$N_e(I_p,t) = N_h(I_p,0)\left[1-\exp\left[-\int_0^t W_k(I_p(t'))\,dt'\right]\right] \qquad (3)$$

where we have denoted the explicit dependence of the transition rate on the time through the irradiance.

An integration over space at the end of the pulse, will give us the number of electrons generated with a given laser pulse:

$$N_e(I_o) = \int_0^{I_o} N_e(I_p,\infty)\,\frac{dV}{dI_p}\,dI_p \qquad (4)$$

where the integral is weighed by the volume that contains that particular irradiance. The integral has an implicit dependence on the density of hydrogen atoms and should not extend beyond the boundary of the atomic hydrogen beam.

The results of the theoretical calculations are shown in Figures 6 and 7 for the range of peak irradiances 1 to 100 TW/cm^2. At low irradiances the electron production was proportional to the third power of irradiance. At irradiances above the "satuation irradiance," where the exponent in Eq. 3 is one, the electron signal did not quite reach the nominal 1.5 power dependence on I_0 that usually occurs for cylindrically symmetric beams. Curiously, although the transition rate predicted by Pindzola et al.[21] and by Reiss[6] contain a plateau at 200 TW/cm^2, the electron production does not reflect the structure in the rates. The cause of this behavior is the rapid depletion of the hydrogen target, and to some extent the contribution to the electron signal from the low irradiance regions within the focal volume. The theoretical results show a difference among the perturbation calculations that is as large as a factor of 3.

The experimental data, corrected for electron gain, transmission of the grids, and solid angle of collection, is displayed in Figure 7 for the production of S_0 electrons. The measured and the calculated numbers due to electrons from other ATI peaks are small and are not included in this discussion. The theory and the measurement were normalized to an atomic hydrogen density of 10^{10} particles/cm^3. The experimental points show a typical division into bunches that we ascribe to the change in the spot size between two distinct sizes. The uncertainty in the irradiance was mostly due to the spot size measurement, and has an error of ±15%. The atomic hydrogen density had an estimated error of ±20%. The electron gain has an error of -15% +20%. The collection efficiency had an error ±5%. The grand total of these errors does not explain the difference between the perturbation theories and the experiment below 10 TW/cm^2. At high irradiance, the break in the curve occurs at 120 TW/cm^2, where the count was 30,000 electrons. If we use the simple rule[12] that at the break $N_e = N_h V_k$, then the atomic hydrogen density would have been 1.1×10^{10} at/cm^3, well within the estimated error in measuring the density.

If we try to match the experiment to the perturbative calculations assuming that a single parameter was measured incorrectly, then a match to the numerical integration calculation[11,21] would occur if the actual irradiance were lower than estimated by a factor of 3. This translates into either the pulse length being longer by 300% or the spot size larger by 17%. These factors are well beyond our estimated uncertainties. If the density, or the electron gain, is assumed to be in error, then the Hydrogen density or the electron gain will have to be lower by a factor of 25, a factor that disagrees with the previous estimate from the saturation break.

However, the different parameters are not independent. The measured irradiance is proportional to W_0^{-2}, while the theoretical production rates, at a given calculated irradiance, are proportional to $\{M^{-2}W_0^{-2}\}$ and hence to W_0^{-3}. Thus an increase in the measured spot radius W_0 by 10% or 20% would reduce the measured irradiance by a factor of .83 or .69 respectively. The calculated signals will also be reduced by .75 or .58 respectively. This small change would match the experiment to the perturbation calculation at low irradiance, but it would cause a disagreement at 100 TW/cm^2.

CONCLUSIONS

The perturbative results are not consistent with our data, overestimating the rates above 1 TW/cm^2. The Coulomb-corrected Keldysh results are in better agreement with measurement. The numerical calculation[11,21] results are different from the measurement, but are within the uncertainties. The Reiss and the Keldysh rates, used by many to predict multiphoton ionization, underestimate the rates by a large factor. The measured spectra are consistent with the prediction that any structure within the total ionization rate would not be seen with our apparatus.

ACKNOWLEDGMENTS

We would like to acknowledge the help of Dr. D. E. Casperson in the design of the electron TOF spectrometer and the help of M. Maestas, K. Stetler, and S. Harper in the lab. This work was performed under the auspices of U.S. Department of Energy under contract W-7405-ENG-36.

REFERENCES

1. L. V. Keldysh, Sov. Phys. JETP 20, 1307-1314 (1965).
2. E. Karule, in Atomic Processes, p.5, Latvian Acad. Sci., Riga (1975) (in Russian).
3. S. V. Khristenko and S. I. Vetchinkin, Opt. Spektrosk. 40, 417 (1976).
4. G. Laplanche, A. Durrieu, Y. Flank, M. Jaouen, and A. Rachman, J. Phys. B. 9, 1263 (1976).
5. A. Maquet, Phys. Rev. A 15, 1088 (1977).
6. H. R. Reiss, JOSA B4, 27 (1987).
7. S. I. Chu and J. Cooper, Phys. Rev. A32, 2769 (1985).
8. H. R. Reiss, Phys. Rev. A22, 1786-1813 (1980).
9. B. Gao and A. F. Starace, Phys. Rev. Lett. 61, 404 (1988).
10. B. Gao and A. F. Starace, Phys. Rev. A39, 4550 (1989).
11. K. J. Lagattuta, Phys. Rev. A41, 5110 (1990).
12. M. LuVan, G. Mainfray, C. Manus, I. Tugov, Phys. Rev. A7, 91 (1973).
13. D. E. Kelleher, M. Ligare, and L. Brewer, Phys. Rev. A31, 2747 (1985).
14. H. G. Muller, H. B. van Linden van den Heuvell, and M. J. van der Wiel, Phys. Rev. A34, 236-243 (1986).
15. D. Feldmann, B. Wolff, M. Wemhöner, and K. H. Welge, Z. Phys. D 6, 293-294 (1987). B. Wolff, H. Rottke, D. Feldmann, and K. H. Welge, Z. Phys D 10, 35 (1988).
16. J. P. Roberts, A. J. Taylor, P. H. Y. Lee, and R. B. Gibson, Opt. Lett. 13, 734-736 (1988).
17. P. Kruit and F. H. Read, J. Phys. E: Sci. Inst. 16, 313-324 (1983).
18. J. Slevin and W. Stirling, Rev. Sci. Instrum. 52, 1780-1782 (1981).
19. A. E. Siegman, "Lasers", University Science Books, Mill Valley, California, USA (1986).
20. L. Marshall, Laser Focus, April, pp. 26-28 (1971).
21. M. S. Pindzola, Bull. A.P.S. 35, 1151 (1990); and submitted to Phys. Rev. A.

FIGURE CAPTIONS

1. Simplified energy level diagram of a hydrogen atom showing electron peaks from absorption of three, four, and five 5 eV KrF photons.
2. A schematic diagram of the experimental apparatus. The hydrogen beam points into the page.
3. A schematic diagram of the interaction region. The laser beam is orthogonal to this view.
4. A scan through the laser beam at best focus using a 25 micrometer diameter circular aperture. Measured values are compared to models for 3 spot radii.
5. ATI electron time of flight data for molecular hydrogen (dashed line) at an irradiance of 1.1×10^{14} W/cm^2 in comparison with data for atomic hydrogen (continuous line). Note the atomic hydrogen S1 ATI peak in the molecular hydrogen spectrum. The position matches the pure atomic signal and is not coincident with any background gas ATI peak.
6. The predictions of different theories for the electron production rates at 248 nm by linearly polarized light at a hydrogen density of 10^{10} atoms/cm^3.
7. Comparison of the measurement and the theory.

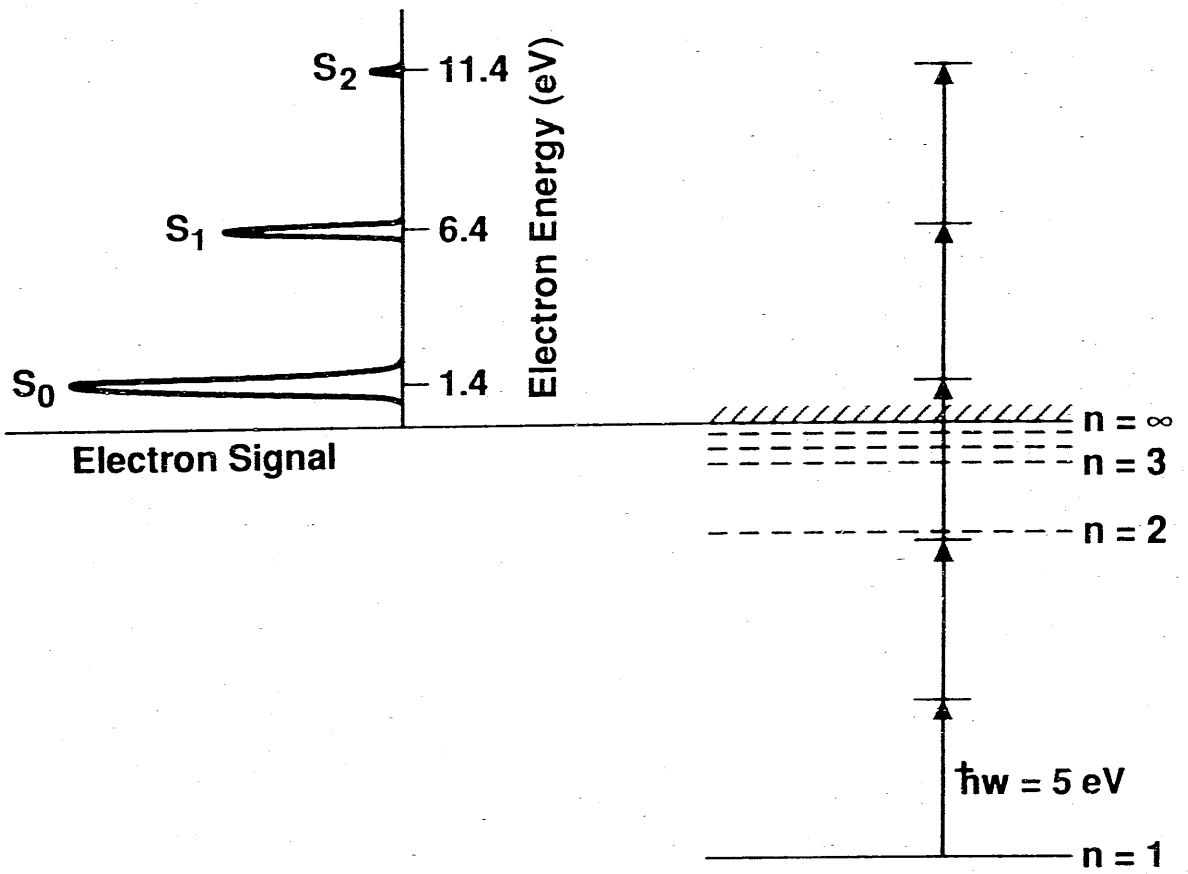
S2
11.4
S1
6.4
S0
1.4
Electron Energy (eV)
Electron Signal
n = ∞
n = 3
n = 2
ħw = 5 eV
n = 1

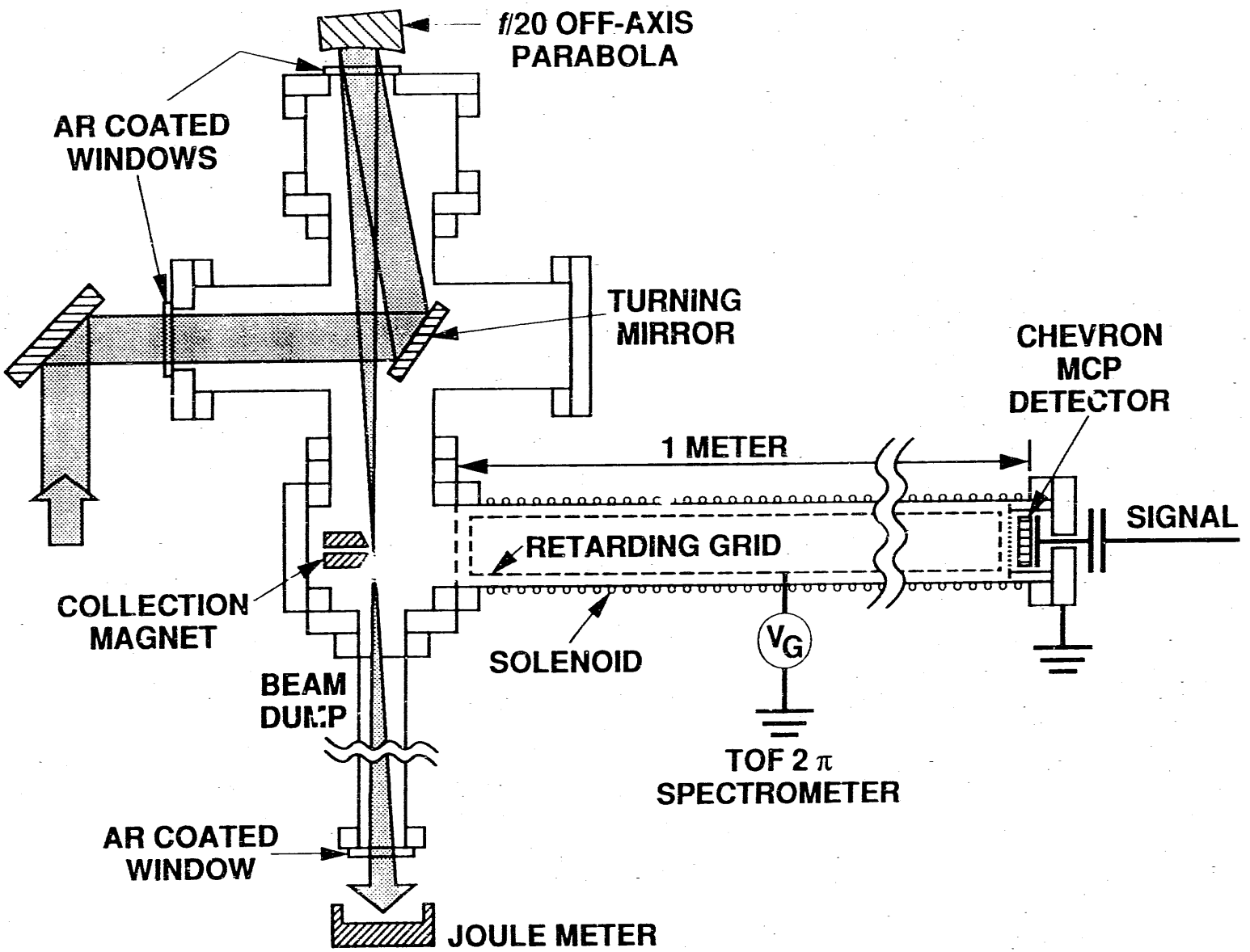
f/20 OFF-AXIS PARABOLA
AR COATED WINDOWS
TURNING MIRROR
CHEVRON MCP DETECTOR
1 METER
SIGNAL
RETARDING GRID
COLLECTION MAGNET
SOLENOID
V_G
BEAM DUMP
TOF 2 π SPECTROMETER
AR COATED WINDOW
JOULE METER

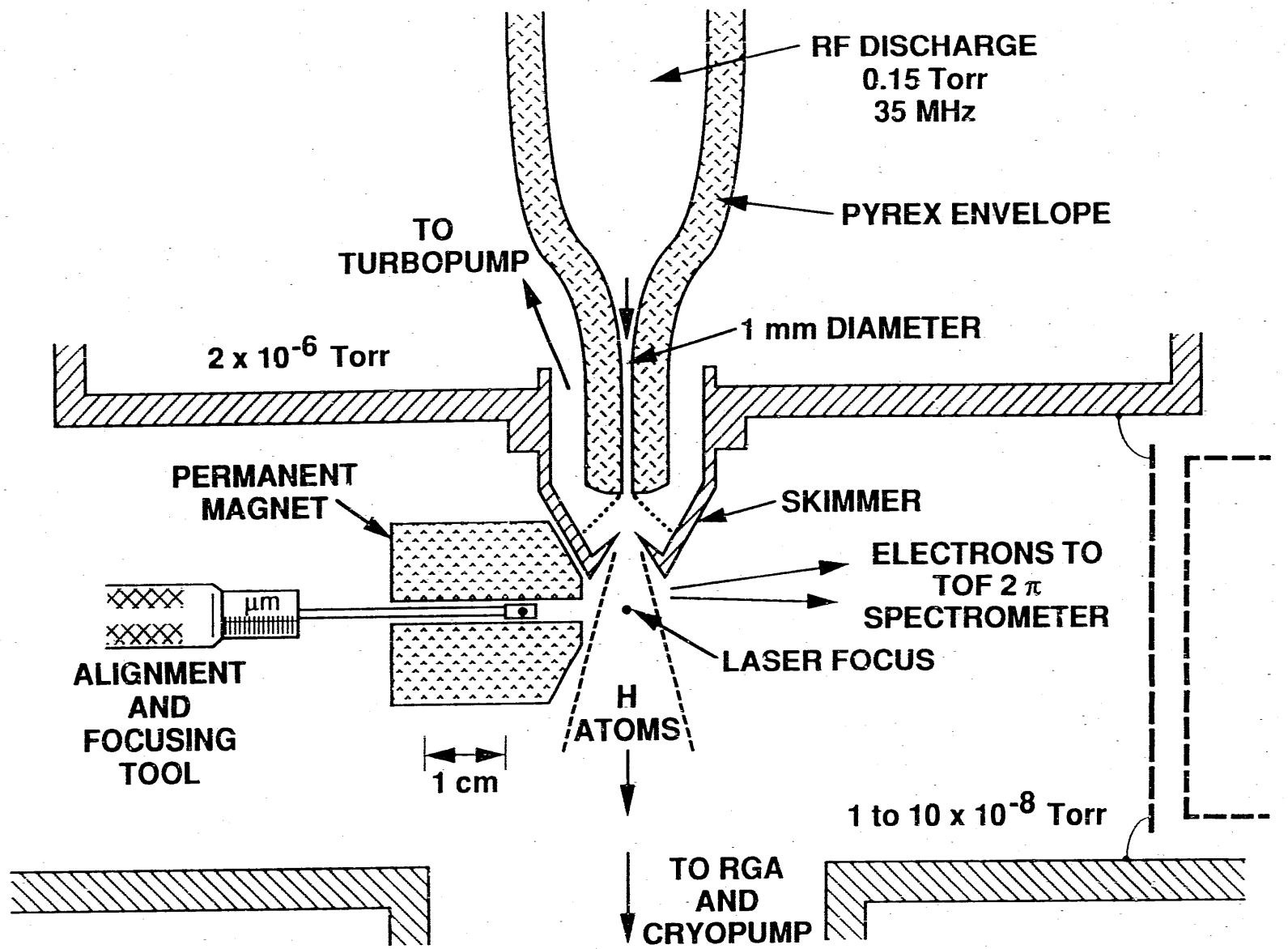
RF DISCHARGE
0.15 Torr
35 MHz
PYREX ENVELOPE
TO
TURBOPUMP
1 mm DIAMETER
2 x 10-6 Torr
PERMANENT
MAGNET
SKIMMER
ELECTRONS TO
TOF 2 π
SPECTROMETER
μm
LASER FOCUS
ALIGNMENT
AND
FOCUSING
TOOL
H
ATOMS
1 cm
1 to 10 x 10-8 Torr
TO RGA
AND
CRYOPUMP

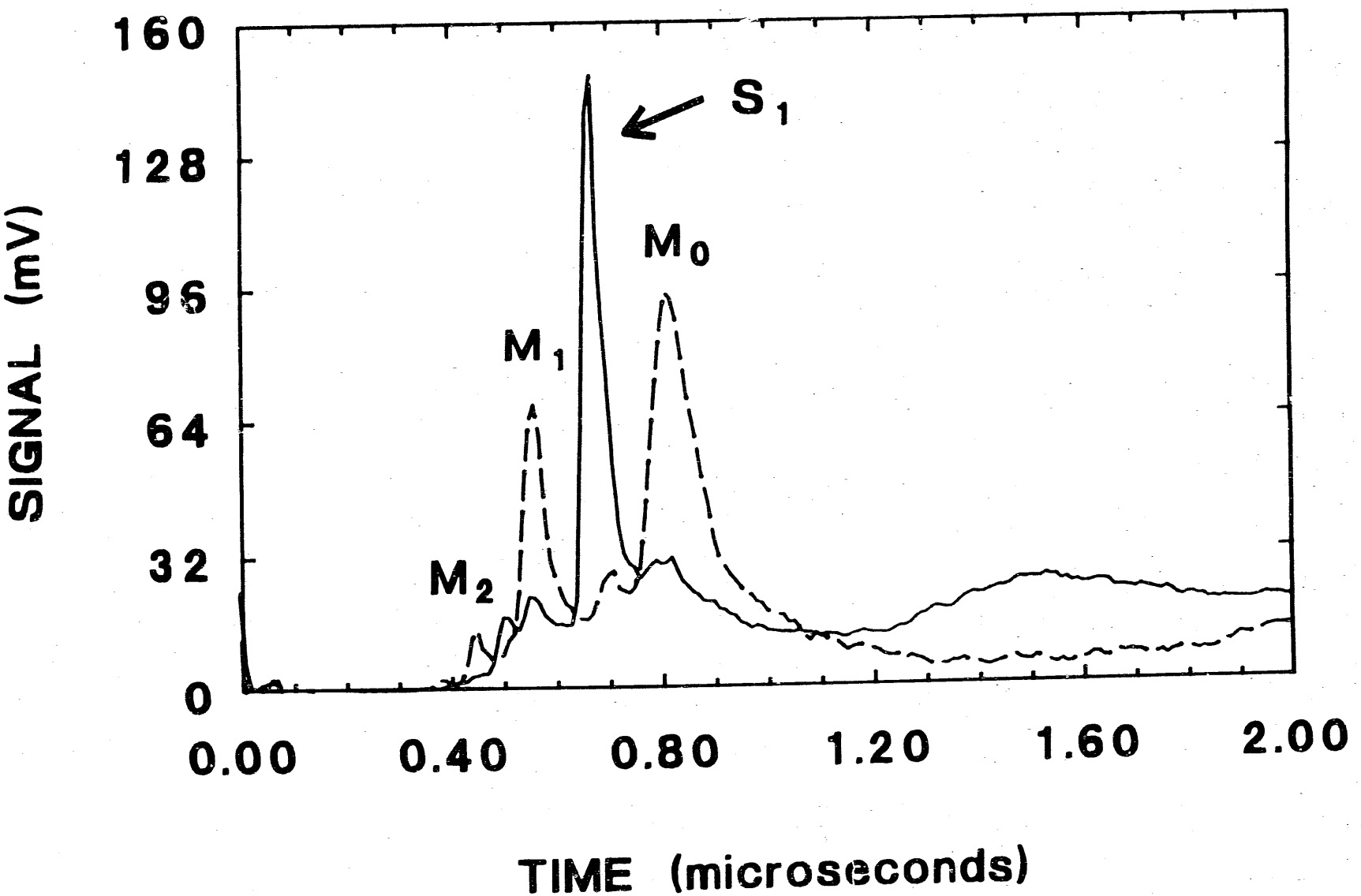
160
128
96
64
32
0
SIGNAL (mV)
S1
M0
M1
M2
0.00
0.40
0.80
1.20
1.60
2.00
TIME (microseconds)

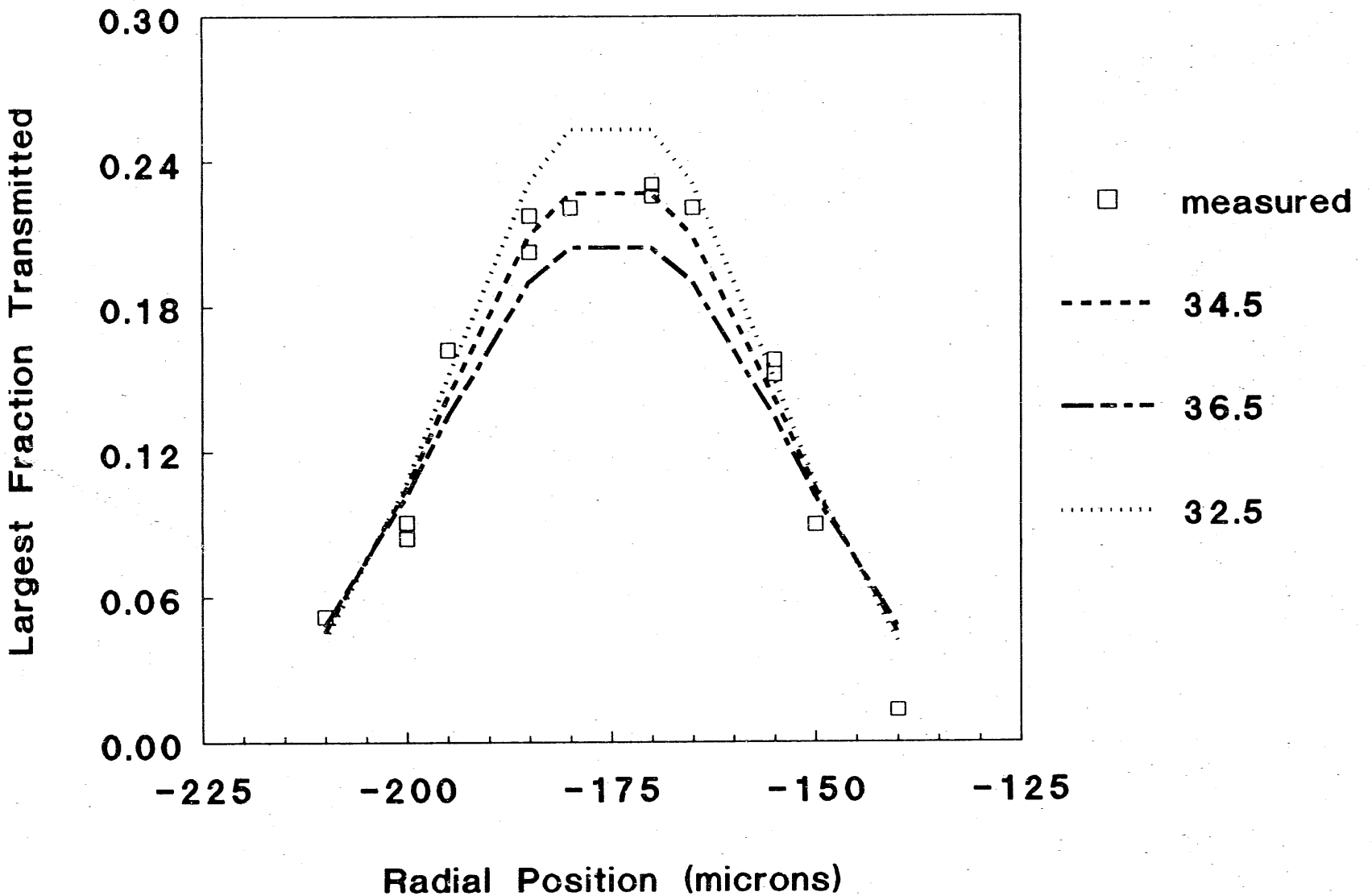
0.30
0.24
0.18
0.12
0.06
0.00
Largest Fraction Transmitted
-225
-200
-175
-150
-125
Radial Position (microns)
measured
34.5
36.5
32.5

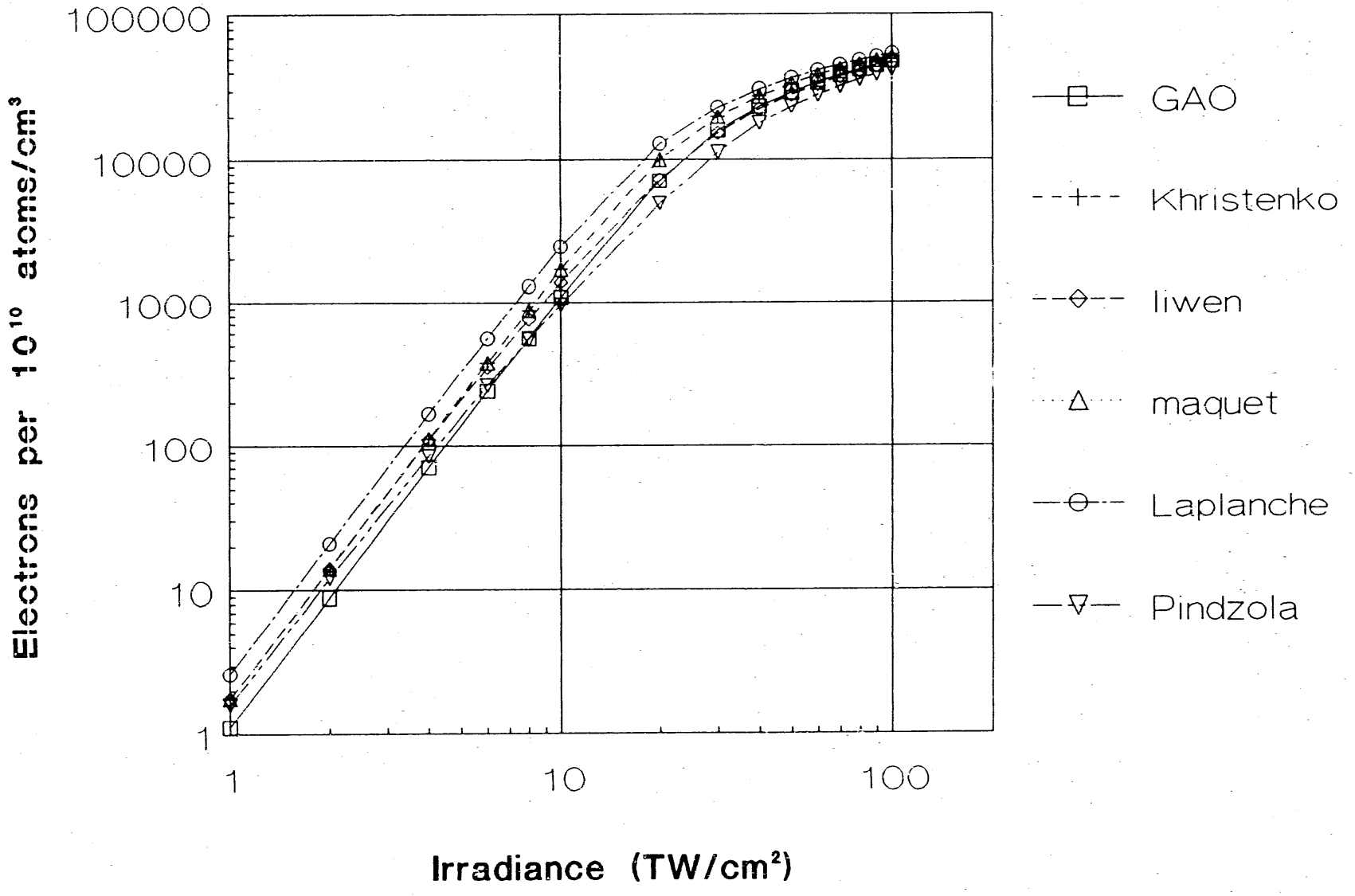
100000
10000
1000
100
10
1
1
10
100
Electrons per 10^{10} atoms/cm^3
Irradiance (TW/cm^2)
GAO
Khristenko
liwen
maquet
Laplanche
Pindzola

THTW1

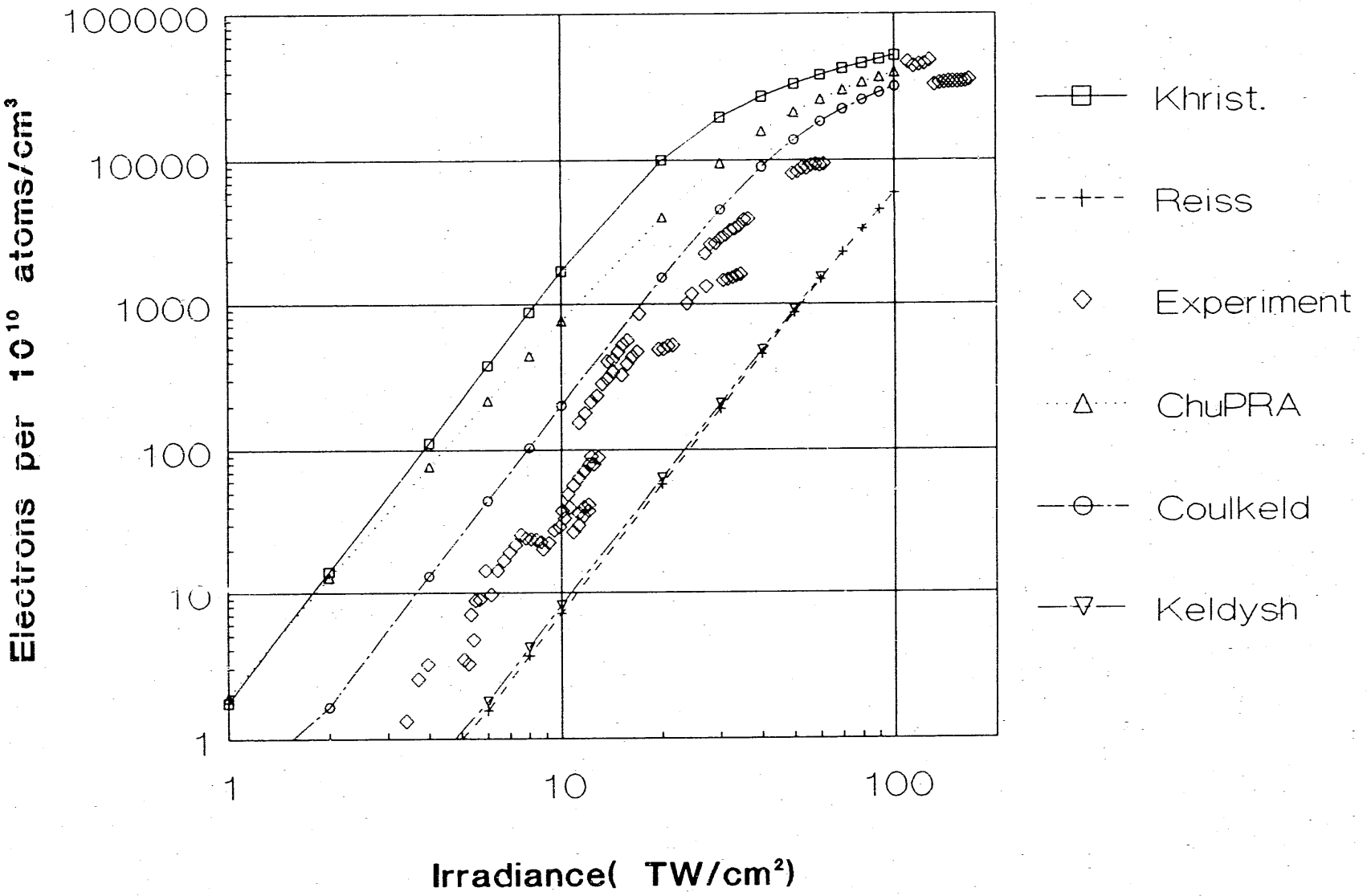
100000
10000
1000
100
10
1
1
10
100
Electrons per 10^{10} atoms/cm^3
Irradiance(TW/cm^2)
Khrist.
Reiss
Experiment
ChuPRA
Coulkeld
Keldysh

TH&m10

-END-

DATE FILMED

11 / 02 / 90